International Journal of Heat and Fluid Flow 31 (2010) 307–314

Contents lists available at ScienceDirect

International Journal of Heat and Fluid Flow

journal homepage: www.elsevier.com/locate/ijhff

Large-eddy simulation of variable-density round and plane jets

Holger Foysi [a,*], Juan P. Mellado [b], S. Sarkar [c]

[a] Aerodynamic Institute, RWTH Aachen, 52062 Aachen, Germany
[b] Institute for Combustion Technology, RWTH Aachen, 52062 Aachen, Germany
[c] Department of Mechanical and Aerospace Engineering, UCSD San Diego, USA

ARTICLE INFO

Article history:
Received 7 September 2009
Received in revised form 25 November 2009
Accepted 2 December 2009
Available online 6 January 2010

Keywords:
LES
Variable-density flow
Round and plane jet
Global instability

ABSTRACT

Large-eddy simulations (LES) of heated and cooled plane and round variable-density jets were conducted using a variety of density ratios $s = \rho_j/\rho_{co}$, which relates the jet nozzle density ρ_j to the freestream density ρ_{co}. The initial momentum flux was kept constant for better comparison of the resulting data. Both simulations confirm experimental results, in that the jet half-width grows linearly with streamwise coordinate x and the lighter jets decay much faster than the heavy ones. The centerline velocity decay is however different between the plane and round geometries. Whereas the round jets exhibits a decay with $1/x$ for all density ratios s, there seem to be two self-similar scalings in plane jets, in the limit of small and large density ratios s. In the limit of small s or for incompressible flow, U_c scales as $U_c \sim 1/\sqrt{x}$, for strongly heated jets on the other hand we find $U_c \sim 1/x$. A mixed scaling is proposed and shown to work nicely for both small and large density ratios s. For the round jet simulations, on the other hand, scaling x and U_c by $s^{-1/4}$ (Chen and Rodi, 1980) collapses the round jet data. Furthermore, it is shown that the streamwise growth in the mean density or the decay of the velocity fluctuations in the quasi-self-similar region, is stronger for round jets. The round jet simulation with a density ratio of $s = 0.14$ is seen to develop under a global instability. To the author's knowledge, this is the first LES of a globally unstable round jet at a density ratio of $s = 0.14$. The frequency agrees excellently with experimental data and with the new scaling proposed by Hallberg and Strykowski (2006).

1. Introduction

Variable-density flows exhibit a range of interesting physical phenomena and arise in a variety of circumstances, e.g. during the mixing process between flows of different densities, during combustion processes or plasma processing. Free shear flows, like jets, are of special interest, due to their application in many industrial devices. However, variable-density jets lack the number of experimental and numerical investigations one finds for jets with constant density. Most experimental studies achieved the density difference by mixing helium and air in various proportions. Ahmed et al. (1985) investigated the discharge of a helium/air mixture into a confined swirling flow. Sreenivasan et al. (1989), Kyle and Sreenivasan (1993) and Panchapakesan and Lumley (1993) performed experiments of round jets of pure helium or air/helium mixtures issuing into the ambient air. Later, Amielh et al. (1996) and Djeridane et al. (1996) studied variable-density turbulent jets of air, helium and CO_2 and more recently Boujemaa et al. (2007) of pure helium, exiting into a low-speed air co-flow. Monkewitz et al. (1989) and Monkewitz et al. (1990) on the other hand, investigated mixing and entrainment of heated transitional round jets. To the authors knowledge, there are only a few numerical simulations available, which investigate variable-density jets. Jester-Zürcker et al. (2005) used Reynolds stress modeling to study the flow inside a non-reactive combustor. Although they were able to obtain good agreement compared to the experiment for a jet with constant density, the modeling showed deficiencies for variable-density flows. LES simulations include the work of LeRibault et al. (1999), Zhou et al. (2001), and Bodony and Lele (2005), who investigated noise emission from heated and unheated jets, Tyliszczak and Boguslawski (2006), Anders et al. (2007), and Wang et al. (2008). The LES simulation of Wang et al. (2008) provided thus far the most detailed comparison between simulation and experiment. They replicated the conditions of Amielh et al. (1996) and Djeridane et al. (1996) to study confined round jets of air, helium and CO_2 exiting into a low-speed air co-flow, and showed excellent agreement between experiment and simulation. When it comes to the plane variable-density jet case, most references consider only slightly heated jets, having density ratios of $s = 0.8$—0.9 (Jenkins and Goldschmidt, 1973; Davies et al., 1975; Bashir and Uberoi, 1975; Antonia et al., 1983; Browne et al., 1984; Ramaprian and Chandrasekhara, 1985), values that do not change the evolution of the jet appreciably. Furthermore, an investigation comparing

* Corresponding author. Tel.: +49 241 80 95188.
E-mail address: h.foysi@aia.rwth-aachen.de (H. Foysi).

0142-727X/$ - see front matter © 2009 Elsevier Inc. All rights reserved.
doi:10.1016/j.ijheatfluidflow.2009.12.001

plane and round jets at various density ratios $s = \rho_j/\rho_{co}$, relating the density at the nozzle exit (indicated by the subscript "j") to that of the co-flow (indicated by the subscript "co"), is lacking. Further insight is however of great interest from a modeling point of view, since it could help to improve our understanding of the so-called round-jet/plane-jet anomaly (Pope, 1978). Experimental data indicates a 15% smaller spreading rate of the round jet than that of the plane jet, whereas numerical simulations used to over-predict the spreading rate of round jets (Magi et al., 2001).

Another import phenomenon observed in variable-density flows is the occurrence of global instabilities (Monkewitz et al., 1990; Kyle and Sreenivasan, 1993; Raynal et al., 1996; Hallberg and Strykowski, 2006; Lesshaft et al., 2006; Nichols et al., 2007), reported to occur if the density ratio s is lower then 0.5—0.6. Above that ratio, the shear-layer fluctuations evolve in a fashion similar to that observed in a constant-density jet, characterized by weak background disturbances. Below that threshold on the other hand, intense oscillatory instabilities may also arise. Since the oscillatory mode was shown to repeat itself with extreme regularity and is subject to strong vortex pairing, abnormally large velocity fluctuations were observed, providing difficulties in numerical simulations. The overall behavior seems not only to depend on the density ratio and the relation of the shear layer thickness to the nozzle width, but also on the Reynolds number, as was recently reported by Hallberg and Strykowski (2006).

The present work aims to present a comparison of selected aspects of round and plane variable-density jets at a variety of density ratios. Furthermore, the simulations are analyzed with respect to the occurrence of a global instability.

2. Details of the simulations

The filtered compressible equations of motion are solved in cylindrical (x, θ, r) or cartesian coordinates for the round and plane jet, respectively, using the compressible form of the dynamic Smagorinsky model (Martin et al., 2000). A top-hat filter was used for test filtering the quantities, as is described in Vreman et al. (1997). Treatment of the centerline singularity at $r = 0$ is accomplished by applying the method of Constantinescu and Lele (2002). There, governing equations for the flow at the polar axis are obtained using series expansions near $r = 0$. For time integration a low-dispersion–dissipation fourth-order Runge–Kutta scheme of Hu et al. (1996) in its low storage form is used. The spatial differentiation utilizes optimized explicit DRP-SBP (dispersion-relation-preserving summation by parts) finite-difference operators of sixth-order (Johansson, 2004). The code employed for the plane jet has been derived from Stanley et al. (2002), and is based on sixth-order compact Padé schemes for space derivatives and a Runge–Kutta fourth-order scheme for time advancement. For numerical stability both simulations require the timestep Δt to be such that the CFL number is restricted by CFL < 1.4. Time accuracy of the solution restricted the CFL number further below CFL $\leqslant 1.1$ (Popescu et al., 2005). This numerical scheme yields numerical errors that are small compared to the subgrid-scale terms of the governing equations when the filter size is chosen as twice the grid size (Chow and Moin, 2003), as it is done here. Tables 1 and 2 give an overview over the different simulation parameters.

The initial momentum flux m_j has been fixed for all simulations and was chosen similarly as in Wang et al. (2008). This reasoning was based on observations of Ricou and Spalding (1961), who showed that the entrainment rate of a jet strongly depends on m_j. Ruffin et al. (1994) demonstrated additionally, that the Taylor and Kolmogorov length scales are determined by the initial momentum flux. This reasoning was adopted, too, by other experiments and simulations, for example Amielh et al. (1996), Djeridane et al. (1996), and Wang et al. (2008). Non-reflecting boundary conditions (Lodato et al., 2008) were applied, together with a combination of grid stretching and spatial filtering close to the boundaries to damp disturbances. A constant grid spacing was chosen within the range $0 < r/r_j,\ |z/h| < 1.5$ and $0 < x/r_j < 12$, where h denotes half the slot width D of the plane jet. A subsequent relative stretching of 1% was used extending in the r, z-direction up to $r/r_j,\ z/h = 12$ and up to $x/r_j = 50$ and $x/h = 42$ in the streamwise direction, for the round and plane jet simulations, respectively. In the remaining part of the domain the stretching ratio was increased to 5%. The number of grid points within $0 \leqslant r/r_j,\ z/h \leqslant 1$ was 11. The LES simulation where run using 16 processors on the JUMP supercomputer of the Jülich Supercomputing Centre, with a CPU time of approximately 24 h, including statistics. The round jet simulations were initialized using velocity profiles of the form (Bodony and Lele (2005))

$$U = U_{co} + \frac{1}{2}(U_j - U_{co})\left(1 - \tanh\left[\left(\frac{r}{r_j} - \frac{r_j}{r}\right)\frac{1}{4\delta_{\theta 0}}\right]\right),$$

and temperature fields using the Crocco–Busemann relation (Chassaing et al., 2002). For the plane jet similar profiles were applied (replace r_j with $D/2$ and r with z), making use of the symmetry at $z = 0$. The initial normalized momentum thickness in the above profiles was prescribed. To trigger the transition to turbulence precursor simulations of annular and plane temporally evolving mixing layers with smaller initial momentum thickness were performed for the round and plane jet problem, respectively. The square root of the turbulent kinetic energy was monitored until its value $\sqrt{(U')_1^2 + (U')_2^2 + (U')_3^2}$, non-dimensionalized using the mean values at the jet inlet, was of the order of 0.05 and the mean velocity profiles agreed closely with the prescribed inlet mean jet profiles. The resulting fluctuations were convected into the fluid domain using the characteristic inflow boundary conditions. Additionally, solenoidal broadband velocity fluctuations (Stanley and Sarkar, 2000) and stochastic vortex ring perturbations (Bogey and Bailly, 2003) were superimposed on the plane and annular mixing layer, respectively, to break the periodicity of the inflow data. Although the domain sizes and number of grid points are similar to the ones chosen by Bodony and Lele (2005), the grid resolution was checked by performing two simulations at higher resolution ($n_x \times n_\theta \times n_r = 384 \times 80 \times 120$) for cases R152 and R014, too. These simulations showed

Table 1
Parameters of the plane jet LES simulations. $\delta_{\theta 0}/D$ denotes the initial momentum thickness and L_i the domain lengths, normalized by the jet diameter D and $h = D/2$, respectively. $Re = U_j\rho_j D/\mu_j$ is not available here, since the resolved viscous terms are negligible compared to the viscous subgrid terms and were neglected. The number of grid points in streamwise, spanwise and cross-stream direction are n_x, n_y and n_z, respectively.

Case	Re	$D/\delta_{\theta 0}$	s	L_x	L_y	L_z	n_x	n_y	n_z
P013	N/A	10	0.125	52	24	32	192	96	160
P080	N/A	10	0.8	52	24	32	192	96	160
P100	N/A	10	1.0	52	24	32	192	96	160

Table 2
Parameters of the round jet LES simulations. The domain lengths L_i were normalized by r_j and $\delta_{\theta 0}/D$ denotes the initial momentum thickness, normalized by the jet diameter D. The Reynolds number is given as $Re = U_j\rho_j D/\mu_j$. The number of grid points in the respective coordinate directions are represented by n_i.

Case	Re	$D/\delta_{\theta 0}$	s	L_x	L_θ	L_r	n_x	n_θ	n_r
R014	7000	27	0.14	60	2π	16	256	64	112
R100	21000	27	1.00	60	2π	16	256	64	112
R152	32000	27	1.52	60	2π	16	256	64	112

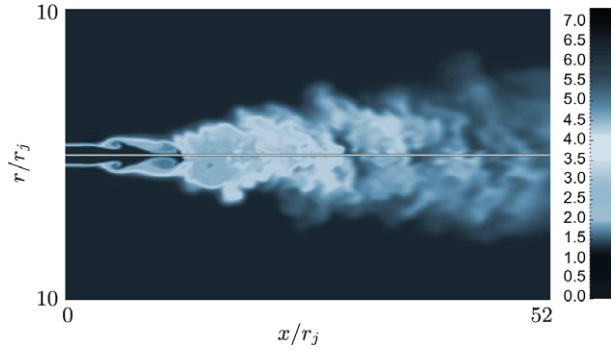

Fig. 1. Contour plot of the density ρ/ρ_j for case R014.

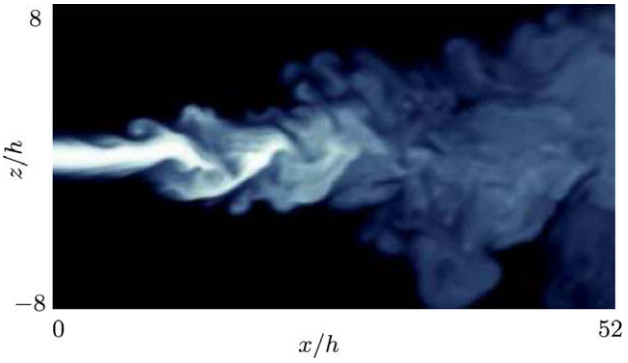

Fig. 2. Contour plot of the density ρ/ρ_j for case P013. Color table similar to Fig. 1.

negligible differences regarding the statistics presented in this paper.

The statistical quantities were obtained by averaging in the homogeneous directions and over a time period T, corresponding to a Strouhal number $D/(TU_j) = 9 \times 10^{-4}$, after statistical stationarity was reached. Figs. 1 and 2 demonstrate the jet development for the round and plane jet cases R014 and P013, respectively, showing contour plots of the density ρ/ρ_j.

3. Comparison of statistical values

3.1. Profiles along the jet axis

Fig. 3 shows the mean velocity difference $\Delta U = \bar{U} - U_{co}$ normalized by the jet half-width (position at which the streamwise velocity dropped to half the centerline value) at various streamwise positions for cases R014 and R100. All profiles for the round jet collapse nicely, indicating self-similar behavior. They furthermore agree well with an exponential of the form $U = \exp[-(r/\delta_h)^2 \ln 2]$. Similarly to the round jet cases, we observe a collapse of the streamwise velocity difference for the plane jet cases P013 and P100 at various x-locations and for different density ratios, too (Fig. 4). The decay of the centerline velocity U_c of variable-density jets has been investigated by many researches, before. No *general* similarity solution may be found for plane jets, as pointed out by Mellado (2004). For incompressible flow and low variable-density flow, dimensional analysis and conservation of momentum suggests that $U_c/U_j \sim \sqrt{h/x}$. Fig. 5, which shows the centerline velocity decay for the plane jet LES simulations, confirms this relationship. In agreement with data from the literature, one observes that lighter jets decay much faster than heavy jets, owing to the conservation of streamwise momentum. Nevertheless, the high density variability prohibits a collapse of the data. For the variable-density cases, however, in terms of dimensional analysis, in

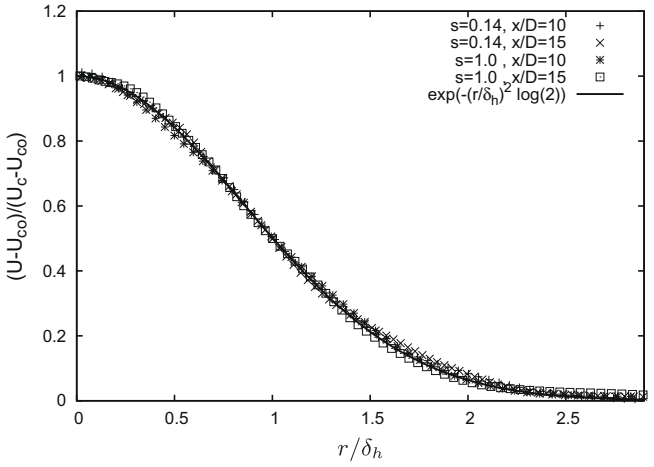

Fig. 3. Normalized radial distribution of the velocity difference at various streamwise locations versus the radial distance normalized by the jet half-width δ_h for the LES round jet cases R014 and R100.

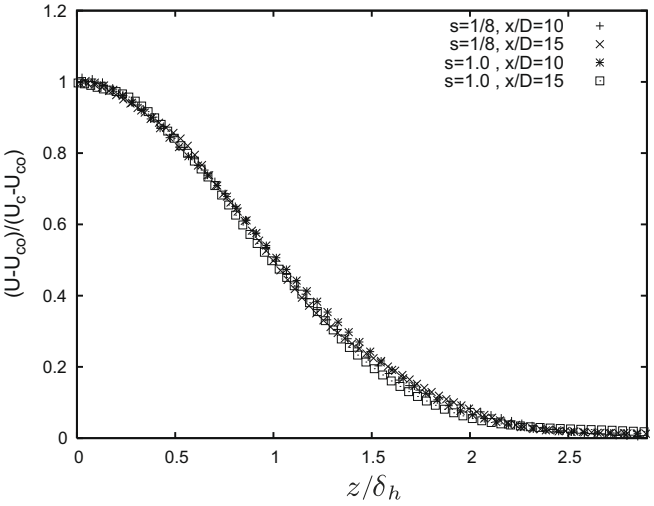

Fig. 4. Normalized cross-stream distribution of the velocity difference at various streamwise locations versus the cross-stream distance normalized by δ_h for the LES plane jet cases P013 and P100.

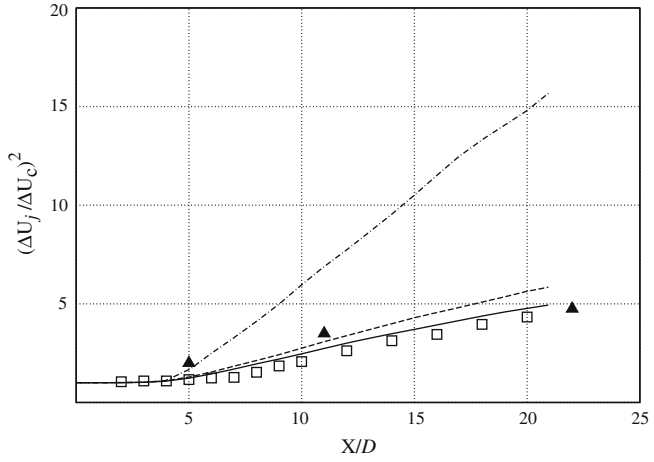

Fig. 5. Centerline velocity decay for the plane jet LES results. —$s = 1$, – – –$s = 0.8$, –. –. –$s = 1/8$, □ Browne et al. (1983) and ▲ Ramaprian and Chandrasekhara (1985).

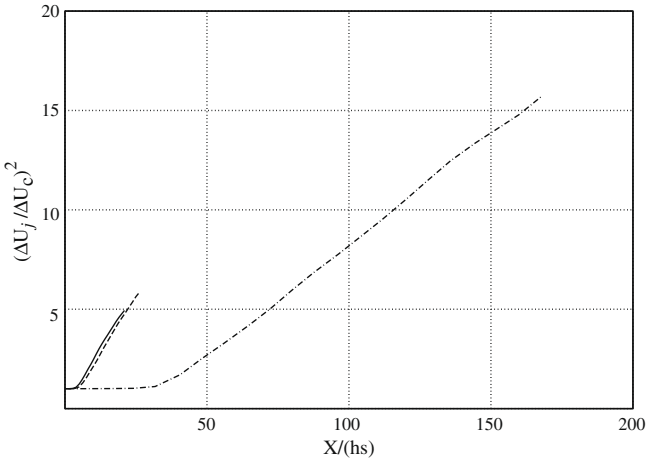

Fig. 6. Centerline velocity decay for the plane jet LES results, using the effective nozzle width *hs*. —$s = 1$, – – –$s = 0.8$, –. – .$s = 1/8$.

addition to the group of parameters $(x, m_j, /\rho_{co})$, m_j being the momentum flux of the jet, now the flux of heat, m_T, and the co-flow temperature, T_{co}, have to be included, and the parameters are no longer independent. However, two limiting self-similar cases can be identified. One situation in which there is self-similar behavior, first considered by Thring and Newby (1953), is the Boussinesq limit, $\Delta\rho \ll \rho$, which is reached eventually far enough downstream. Dimensional analysis then yields $U_c/U_j \sim \sqrt{sh/x}$. This relation is tested in Fig. 6 and shows that there is indeed a collapse for the data with low s only, if x is scaled with the density ratio s. A second self-similar solution that exists in the other limit, namely, a strongly heated jet, would depend on the group of parameters $(x, T_{co}, m_j/(\rho_j T_j), m_T/(\rho_j T_j))$, rendering it difficult to obtain a simple scaling law. However, if $\Delta T \gg T_{co}$, then T_{co} drops from the problem and the solution solely depends on $(x, m_j/(\rho_j T_j), m_T/(\rho_j T_j))$. Dimensional analysis finally gives for the jet velocity and temperature half-widths (δ_h, δ_T, location where the respective values reached half the centerline values)

$$\begin{aligned} &\tfrac{\delta_h,\ \delta_T}{x} = constant, \\ &\tfrac{U_c}{m_T/(\rho_j T_j x)} = constant \ \Rightarrow\ \tfrac{U_c}{U_j} \sim \tfrac{h}{x}, \\ &\tfrac{T_c}{m_T^2/(m_j \rho_j T_j x)} = constant \ \Rightarrow\ \tfrac{T_c}{T_j} \sim \tfrac{h}{x}, \end{aligned} \tag{1}$$

with δ_h being the jet half-width. This shows that for high s the density itself evolves as $\rho_c/\rho_j \sim x/D$, since $\rho \propto 1/T$ for the current flows, where the pressure is almost constant. Note that, in this limit, s does not appear in the final expressions and the centerline values decay hyperbolically with the downstream distance, faster than in the isothermal jet (Fig. 5).

In principle, these two sets of self-similar solutions are independent of each other, but they can be approximately reduced to one scaling in the following way. Under self-similarity, conservation of momentum flux yields

$$\frac{\rho_c U_c^2 \delta_h}{\rho_j U_j^2 h} \sim constant, \tag{2}$$

where the constant depends on the shape of the self-similarly scaled velocity and density profiles. Since $\delta_h \sim x$, independently of s as will be shown below, we finally have

$$U_c/U_j \sim \sqrt{\frac{h\rho_j}{x\rho_c}}. \tag{3}$$

This mixed scaling therefore should cover both limits, in basically using the centerline density ρ_c instead of ρ_{co}. Indeed, as predicted from theory, Fig. 7 shows the desired collapse of the profiles for the plane jet simulations when using the mixed scaling, whereas the previously used scalings were not able to collapse all the data, as could be seen in Figs. 5 and 6.

The centerline velocity decay of the round jet case R014, along with data of Wang et al. (2008) and the similarity law proposed by Chen and Rodi (1980)

$$U_c/U_j = 6.3(\rho_j/\rho_{co})^{1/2}(2r_j/x), \tag{4}$$

is shown in Fig. 8. Although the simulations of Wang et al. (2008) calculated confined jets using fully developed pipe flow as inlet condition, the agreement is very good. As a further check, the normalized radial distribution of the streamwise velocity fluctuations at various streamwise locations versus the radial distance are depicted in Fig. 9. The simulations show fair agreement and a collapse of the data is observed, when normalized using the centerline velocity and the jet half-width. Using the same mixed scaling as proposed for the centerline velocity decay of the plane jet did not collapse the data for the round jet cases (not shown here). Here the centerline velocity is depicted in Fig. 10 using the Witze scaling (Witze, 1974), which is used to obtain a common potential core collapse location x_c and include Mach number effects. The collapse location x_c is gi-

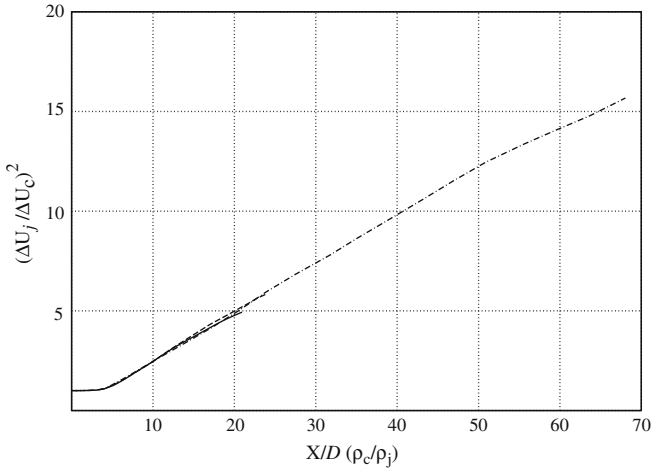

Fig. 7. Centerline velocity decay for the plane jet LES results, using the centerline density. —$s = 1$, – – –$s = 0.8$, –. – .$s = 1/8$.

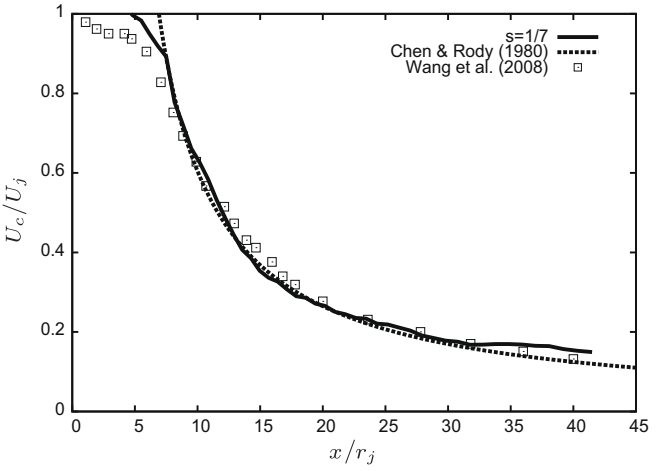

Fig. 8. Centerline velocity decay for case R014, compared to data of Wang et al. (2008) (CH_4) and the scaling law of Chen and Rodi (1980).

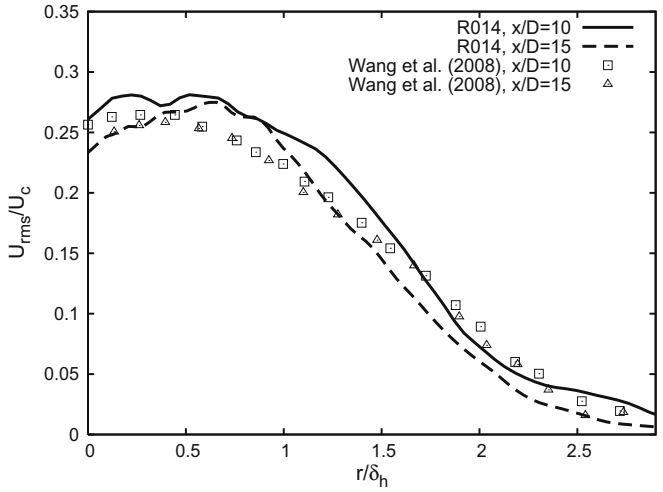

Fig. 9. Normalized radial distribution of the streamwise velocity fluctuations at various streamwise locations versus the radial distance, compared to data of Wang et al. (2008).

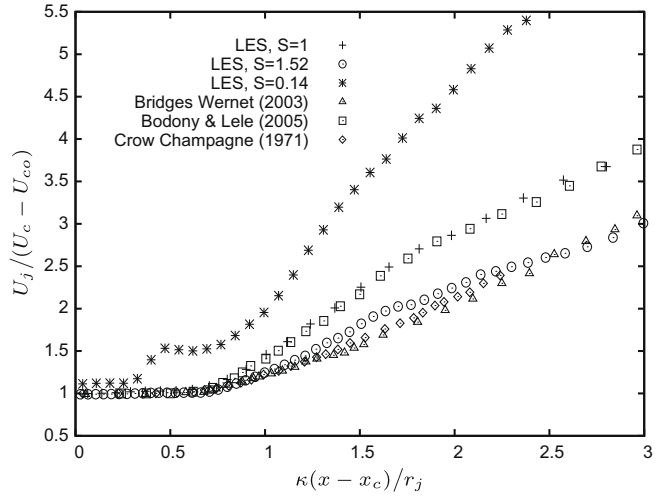

Fig. 10. Inverse centerline streamwise velocity decay of the round jet using the Witze scaling (Witze, 1974).

ven as $x_c/r_j = 0.7[\kappa^2/s]^{-1/2}$, where $\kappa = 0.08(1 - 0.16M_j)s^{-0.22}$. The simulations are compared with data from (Crow and Champagne, 1971; Bridges and Wernet, 2003; Bodony and Lele, 2005) at $s = 0.95$ (Bridges and Wernet, 2003; Bodony and Lele, 2005) and $s = 1$ (incompressible Crow and Champagne, 1971). The observed linear growth of $1/U_c$ with x agrees with the prediction of self-similar analysis (So, 1986), although several assumptions are made, including that of a constant Chapman–Rubesin parameter. As already mentioned by Bodony and Lele (2005), the incompressible data decays slower than that of the numerical simulations, presumably due to a mismatch in initial conditions. A better collapse of the data is obtained by using the analysis of Chen and Rodi (1980). They expressed the velocity decay using a downstream distance parameter x^* and centerline velocity U_c^*, defined by

$$x^* = s^{-1/4}x \tag{5}$$

$$U_c^* = s^{-1/4}U_c. \tag{6}$$

Fig. 11 shows that, contrary to the plane jet case were a mixed scaling worked, the scaling proposed by Chen and Rodi (1980) is required to collapse the data in the round jet case.

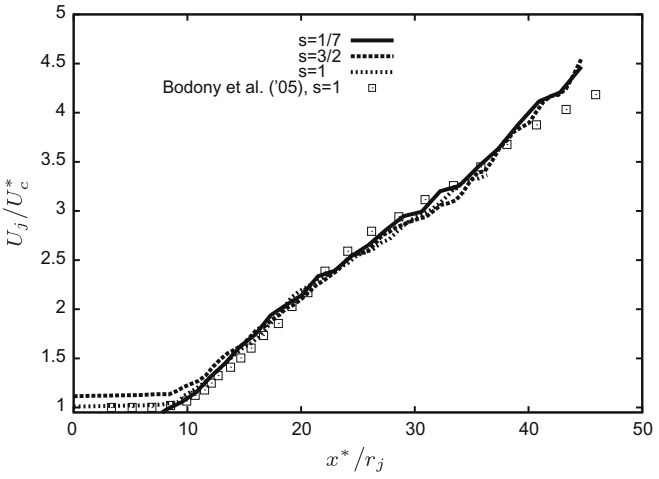

Fig. 11. Centerline velocity decay using $U_c^* = s^{-1/4}U_c$ and $x^* = s^{-1/4}(x - x_s)$. The streamwise coordinate was shifted using the virtual origin x_s.

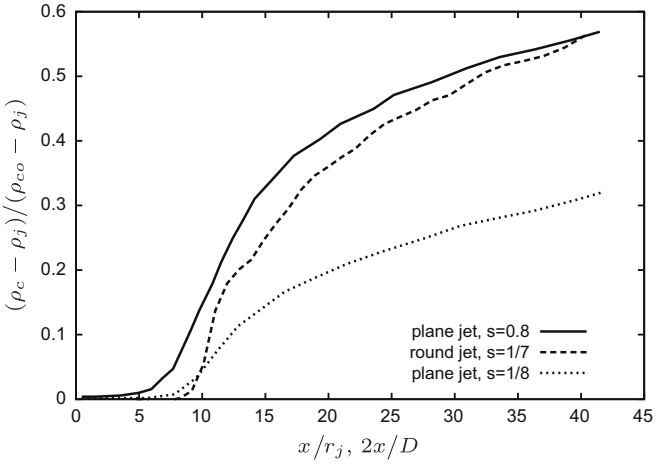

Fig. 12. Growth of centerline density $(\rho_c - \rho_j)/(\rho_{co} - \rho_j)$ for case R014, compared to the plane jet LES cases with $s = 1/8$ and $s = 0.8$. D is the slot width.

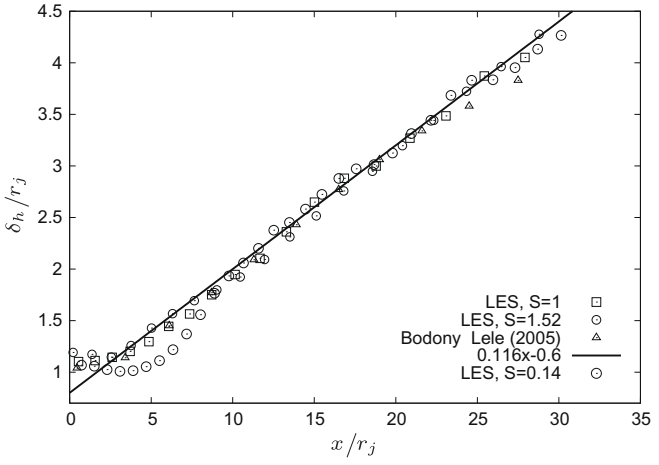

Fig. 13. Streamwise evolution of the round jet half-width δ_h, shifted by using the virtual origin x_s.

The development of the centerline density is seen in Fig. 12, for the round jet case with $s = 1/7$ and the plane jet cases with $s = 0.8,\ 1/8$. Both, plane and round jets, first show only minor

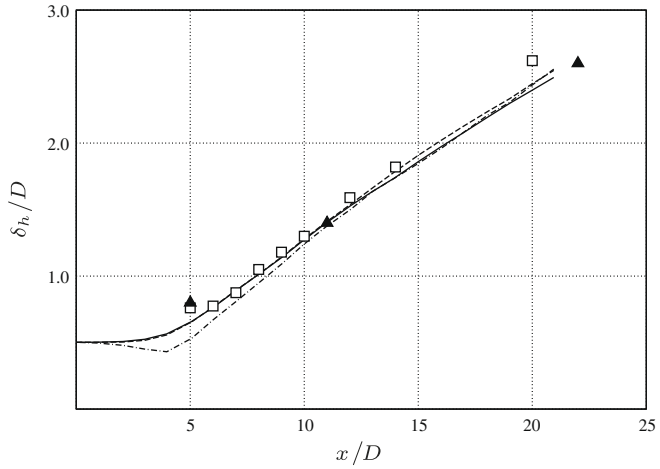

Fig. 14. Streamwise evolution of the plane jet half-width, δ_h, in the LES: $s = 1$, $s = 0.8$, $s = 1/8$. Experimental data: □ Browne et al. (1983) and ▲ Ramaprian and Chandrasekhara (1985).

mixing before strong nonlinear growth occurs. As reported by Mellado (2004), after this nonlinear growth phase the jet density continues to increase almost linearly for case $s = 1/8$. Self-similar analysis predicts this mean density linear regime for strongly heated jets, before the core density reaches values comparable to the co-flow; beyond that point, temperature becomes a passive scalar if no buoyancy is present. The round jet centerline density grows faster, but starts to increase slightly further downstream than the plane jet simulations. This seems to be caused by the strong global instability, to be discussed below, and slightly different initial conditions. The stronger growth in simulation R014 compared to the plane jet simulations could be expected, however, due to the larger surface undergoing turbulent mixing relative to the plane jet.

The different growth rates observed for the inverse centerline velocity decay $1/U_c$ with respect to the magnitude of the density ratio s, are not seen when looking at the jet half-width. Linear growth with x is observed as depicted in Figs. 13 and 14, with a similar magnitude of the half-width for plane and round jets, of 0.112 versus 0.116, respectively. The round jet data is compared with a simulation from Bodony and Lele (2005) at $s = 0.95$, the plane jet data with experiments from Browne et al. (1983) and Ramaprian and Chandrasekhara (1985), showing fairly good agreement. Note, that the data was shifted using the virtual origin x_s, to illustrate that the growth rate is the same within the round or plane jet data, *irrespective* of the density ratio s. Note, that case R014 deviates initially, which seems to be caused by the strong oscillations observed in the streamwise velocity in this region. Fig. 15 shows a comparison of the streamwise evolution of the radial Reynolds stress component (round jet) and cross-stream Reynolds stress component (plane jet, other components show similar trends). Interestingly, the peak values among the simulations with similar density ratio s are of the same order of magnitude. However, with increasing density ratio s higher peak Reynolds stresses are observed, which is consistent with results from Djeridane et al. (1996), showing the same trend. The initial growth for the round jet cases is delayed, but it is possible, by using the Witze scaling, to collapse the profiles in the early development region. As observed for the mean density growth, during the self similar stage a different evolution of round and plane jets is obvious here, too. The peak is more pronounced for the round jet simulations, with a stronger decrease thereafter.

3.2. Global instability

In case R014, high amplitude oscillations were observed, especially for the streamwise velocity and density, leading to strong gradients which made the simulation unstable at first. Adding artificial dissipation (Fiorina and Lele, 2007) helped stabilizing the calculation. This strong oscillating mode together with the strong vortex pairing events as well as the occurrence of side jet phenomena points toward the existence of a global instability in this simulation. Evidence for this is shown in Fig. 16, plotting the power spectrum of the streamwise velocity at various streamwise locations. The power spectrum clearly shows the fundamental frequency and its sub-harmonics at various streamwise positions (shifted for better visibility). The peak is clearly visible until a sudden transition to turbulence has occurred around $x/D = 7$. The Strouhal number of this oscillating mode $St_D = fD/U_j$ was calculated and compared to various experimental datasets, depicted in Fig. 17. Excellent agreement is seen between the simulation results and the experimental data. For the plane jet simulations no such global mode was observed, neither in the DNS nor the LES simulations. After Hallberg and Strykowski (2006), the global oscillations depend on the density ratio s, $D/\delta_{\theta 0}$ and the Reynolds number, as

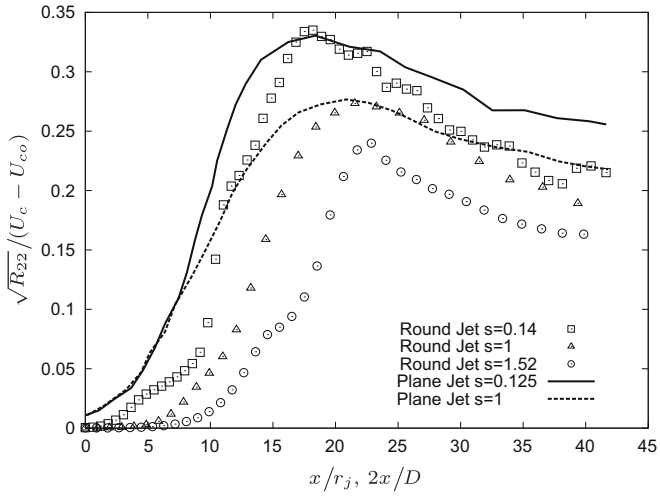

Fig. 15. Streamwise evolution of the centerline cross-stream Reynolds stress normalized using the centerline velocity difference, taken from the LES results.

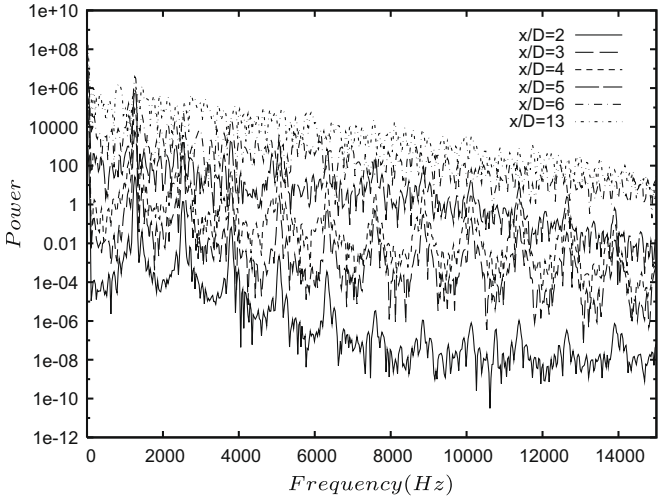

Fig. 16. Frequency power spectrum of the stramwise velocity at various streamwise positions (curves shifted for better visibility).

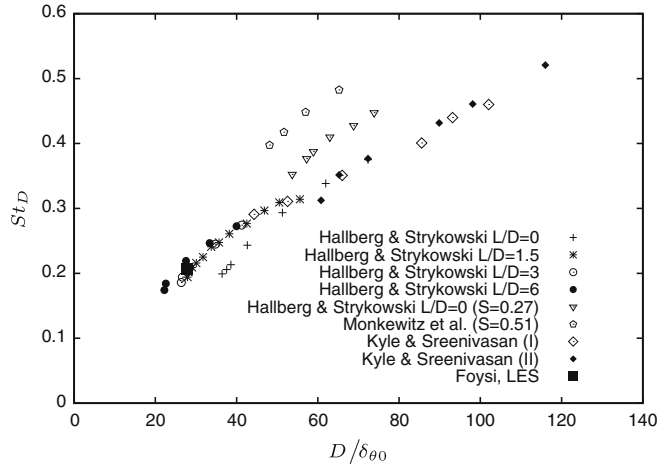

Fig. 17. Strouhal number of the global instability mode, compared with experimental data. The experiments of Hallberg and Strykowski (2006) were conducted with extension tubes of different lengths L/D.

long as compressibility and buoyancy effects are unimportant. Going further than Kyle and Sreenivasan (1993) and Hallberg and Strykowski (2006) non-dimensionalize the frequency by the *viscous* time scale D^2/ν, thus retaining the Reynolds number in the frequency dependence. They were then able to collapse all data onto a straight line, when plotting the Roshko number fD^2/ν over $Re\sqrt{D/\delta_{\theta 0}}(1+\sqrt{s})$. Using the scaling of Hallberg and Strykowski (2006), the LES result of case R014 is plotted along with other variable-density jet data in Fig. 18. Again, excellent agreement is found and the data almost collapses onto a single line. Interestingly, Amielh et al. (1996), Djeridane et al. (1996) in their experiments and Wang et al. (2008) in their simulations did not observe this oscillating mode. A reason for this behavior was first suspected to be caused by differences in the inflow conditions, which serve to trigger the transition to turbulence, or in the different Mach number used in our simulation, which is $M_j = 0.2$ and therefore higher than that of the experiments replicated by Wang et al. (2008). However, Raynal et al. (1996) showed in their measurements and stability calculations, that the relative position of the inflection points of the velocity and density profiles influences strongly the stability of the flow under investigation. The stability of the flow increases by increasing the distance d_i between the two

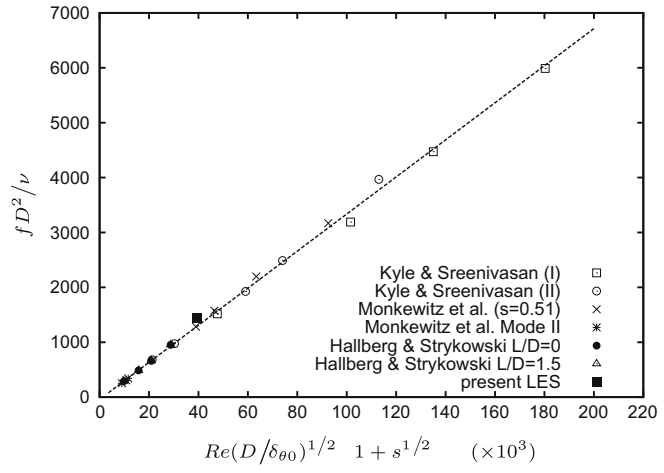

Fig. 18. Roshko number fD^2/ν of the global instability mode, compared with the universal scaling of Hallberg and Strykowski (2006) (L/D denotes the length of the different extension tubes used in the experiments).

inflection points. When comparing helium/air jets to heated jets, they found an increase of the interval d_i in the helium jets. This indicates that the helium jets are consequently more stable than the heated air jets investigated in this paper and might explain the observation of the self-sustained oscillation in simulation R014.

For the plane jet cases, no development under a global mode of instability could be observed. The initial density ratio s and Reynolds number are within the unstable region, required for the occurrence of global modes at a given momentum thickness, as provided by Hallberg and Strykowski (2006) or Raynal et al. (1996). The work of Fulachier et al. (1989) and Monkewitz et al. (1990) indicates, however, that this behavior is observed for particularly clean inflow conditions during the initial stages of turbulence. It is likely that the broadband inflow forcing used for the plane jet simulations inhibits the occurrence of global modes due to the rapid transition to fully developed turbulence. This issue is subject to current investigations in our group.

4. Conclusions

Results of LES simulations of round and plane jets at various density ratios, ranging from $s = 0.125$ to $s = 1.52$ have been presented. The streamwise linear growth of the round and plane jet half-width was found to be of similar magnitude, with slightly lower growth of the plane jets and independent of the density ratio s, as reported in the literature. The centerline velocity decay rates are strongly affected by heating and exhibit different behavior for round and plane jets. Whereas the round jets exhibits a decay with $1/x$ for all density ratios s, there are two self-similar scalings found in plane jets, in the limit of low and high variable-density flow. In the limit of small s or for incompressible flow, U_c scales as $U_c \sim 1/\sqrt{x}$, for strongly heated jets on the other hand we find $U_c \sim 1/x$. A mixed scaling was introduced to work for the range of density ratios considered in this work, which involves the centerline density evolution $U_c \sim \sqrt{\rho_j/(x\rho_c)}$ and transforms into the other scalings in the limit of large and small s. The round jet data, on the other hand, showed different behavior. The quasi-self-similar scaling of Chen and Rodi (1980) was found to collapse the profiles nicely. Chen and Rodi (1980) proposed to account for the density difference by multiplying x and U_c by the factor $s^{-1/4}$. This clearly points to a difference in the development and entrainment process of round and plane jets, which should be taken care of when developing RANS models. Furthermore, it was seen that the streamwise growth in mean density or the decay of the velocity fluctuations in the quasi-self-similar region, after the transition region, is stronger for round jets. The core density reached co-flow values much faster for the round jet and therefore the interval of distances x in which there is a strong density difference between the core and the co-flow is shortened, and it is more difficult to find an intermediate self-similar regime. The round jet data at $s = 0.14$ was seen to develop under a global instability, with the fundamental frequency in excellent agreement with previous experimental data, as summarized by Hallberg and Strykowski (2006). The simulation results confirmed the proposed scaling of Hallberg and Strykowski (2006), who included the Reynolds number dependence of the frequency f by plotting fD^2/ν over $Re(D/\delta_{\theta 0})^{1/2}(1+s^{1/2})$. Such a global mode could not be seen in the plane jet simulations, probably due to the choice of initial conditions.

We believe, that further insight might be found by analyzing the vorticity development and enstrophy budget for both geometries. This, however, requires DNS simulations of the round jet, in order to resolve the small scales appropriately, necessary to reliably interpret the enstrophy budget.

References

Ahmed, S., So, R., Mongia, H., 1985. Density effects on jet characteristics in confined swirling flow. Exp. Fluids 3, 231–238.

Amielh, M., Djeridane, T., Anselmet, F., Fulachier, L., 1996. Velocity near-field of variable density turbulent jets. Int. J. Heat Mass Transfer 39 (10), 2149–2164.

Anders, J., Magi, V., Abraham, J., 2007. Large-eddy simulation in the near-field of a transient multi-component gas jet with density gradients. Comput. Fluids 36, 1609–1620.

Antonia, R.A., Browne, L.W.B., Chambers, A.J., Rajagopalan, S., 1983. Budget of the temperature variance in a turbulent plane jet. Int. J. Heat Mass Transfer 26 (1), 41–48.

Bashir, J., Uberoi, M.S., 1975. Experiments on turbulent structure and heat transfer in a two-dimensional jet. Phys. Fluids 18 (4), 405–410.

Bodony, D., Lele, S., 2005. On using large-eddy simulation for the prediction of noise from cold and heated turbulent jets. Phys. Fluids 17 (8), 85–103.

Bogey, C., Bailly, C., 2003. LES of high Reynolds, high subsonic jet: effects of the inflow conditions on flow and noise. AIAA 2003-3170.

Boujemaa, S., Amielh, M., Chauve, M., 2007. Velocity and concentration distributions in globally axisymmetric helium jets. CR Mecanique 335, 449–454.

Bridges, J., Wernet, M., 2003. Measurements of the aeroacoustic sound source in hot jets. AIAA Paper 2003-3130.

Browne, L.W.B., Antonia, R.A., Rajagopalan, S., Chambers, A.J., 1983. Interaction region of a two-dimensional turbulent plane jet in still air. In: Dumas, R., Fulachier, L. (Eds.), Structure of Complex Turbulent Shear Flows. Springer, pp. 411–419.

Browne, L.W.B., Antonia, R.A., Chambers, A.J., 1984. The interaction region of a turbulent plane jet. J. Fluid Mech. 149, 355–373.

Chassaing, P., Antonia, R., Anselmet, F., Joly, L., Sarkar, S., 2002. Variable Density Fluid Turbulence. Kluwer Academic Publishers.

Chen, C., Rodi, W., 1980. Vertical Turbulent Buoyant Jets: A Review of Experimental Data. Pergamon Press, Great Britain.

Chow, F., Moin, P., 2003. A further study of numerical errors in large-eddy simulations. J. Comput. Phys. 18, 366–380.

Constantinescu, G., Lele, S.K., 2002. A highly accurate technique for the treatment of flow equations at the polar axis in cylindrical coordinates using series expansions. J. Comput. Phys. 183 (1), 165–186.

Crow, S., Champagne, F., 1971. Orderly structure in jet turbulence. J. Fluid Mech. 48, 547.

Davies, A., Keffer, J., Baines, W., 1975. Spread of heated plane turbulent jet. Phys. Fluids 18, 770–775.

Djeridane, T., Amielh, M., Anselmet, F., Fulachier, L., 1996. Velocity turbulence properties in the near-field region of variable density jets. Phys. Fluids 8 (6), 1614.

Fiorina, B., Lele, S.K., 2007. An artificial nonlinear diffusivity method for supersonic reacting flows with shocks. J. Comput. Phys. 222 (1), 246.

Fulachier, L., Borghi, R., Anselmet, F., Paranthoen, P., 1989. Influence of density variations on the structure of low-speed turbulent flows: a report on euromech 237. J. Fluid Mech. 203, 577–593.

Hallberg, M., Strykowski, P., 2006. On the universality of global modes in low-density axisymmetric jets. J. Fluid Mech. 569, 493.

Hu, F., Hussaini, M., Manthey, J., 1996. Low-dissipation and lowdispersion Runge-Kutta schemes for computational acoustics. J. Comput. Phys. 124, 177–197.

Jenkins, P.E., Goldschmidt, V.W., 1973. Mean temperature and velocity in a plane turbulent jet. Trans. ASME: J. Fluids Eng. 95, 581–584.

Jester-Zürcker, R., Jakirlić, S., Tropea, C., 2005. Computational modelling of turbulent mixing in conned swirling environment under constant and variable density conditions. Flow Turbul. Combust. 75, 217–244.

Johansson, S., 2004. High order finite difference operators with the summation by parts property based on DRP schemes. Tech. Rep. 2004-036, it.

Kyle, D., Sreenivasan, K., 1993. The instability and breakdown of a round jet variable-density jet. J. Fluid Mech. 249, 619–664.

LeRibault, C., Sarkar, S., Stanley, S., 1999. Large eddy simulation of a plane jet. Phys. Fluids 11, 3069–3083.

Lesshaft, L., Huerre, P., Sagaut, P., Terracol, M., 2006. Nonlinear global modes in hot jets. J. Fluid Mech. 554, 393.

Lodato, G., Domingo, P., Vervisch, L., 2008. Three-dimensional boundary conditions for direct and large-eddy simulation of compressible viscous flows. J. Comput. Phys. 227 (10), 5105–5143.

Magi, V., Iyer, V., Abraham, J., 2001. The $k-\epsilon$ model and computed spreading rates in round and plane jets. Numer. Heat Transfer Part A: Applicat. 40 (4), 317–334.

Martin, M., Piomelli, U., Candler, G., 2000. Subgrid-scale models for compressible large-eddy simulations. Theor. Comput. Fluid Dyn. 13, 361–376.

Mellado, J.P., 2004. Large-eddy simulation of variable density flows. Ph.D. Thesis, UCSD San Diego.

Monkewitz, P., Lehmann, B., Barsikow, B., Bechert, D., 1989. The spreading of self-excited hot jets by side jets. Phys. Fluids A 1, 446–448.

Monkewitz, P., Bechert, D., Barsikow, B., Lehmann, B., 1990. Self-excited oscillations and mixing in a heated round jet. J. Fluid Mech. 213, 611.

Nichols, J., Schmid, P.J., Riley, J., 2007. Self-sustained oscillations in variable-density round jets. J. Fluid Mech. 582, 341–376.

Panchapakesan, N., Lumley, J., 1993. Turbulence measurements in axisymmetric jets of air and helium. Part 1. Air jet. J. Fluid Mech. 246, 197–223.

Pope, S., 1978. An explanation of the turbulent round-jet/plane-jet anomaly. AIAA J. 16 (3), 279–281.

Popescu, M., Shyy, W., Garbey, M., 2005. Finite volume treatment of dispersion-relation-preserving and optimized prefactored compact schemes for wave propagation. J. Comput. Phys. 210 (2), 705–729.

Ramaprian, B.R., Chandrasekhara, M.S., 1985. Lda measurements in plane turbulent jets. Trans. ASME: J. Fluids Eng. 107, 264–271.

Raynal, L., Harion, J.-L., Favre-Marinet, M., Binder, G., 1996. The oscillatory instability of plane variable-density jets. Phys. Fluids 8, 993.

Ricou, F., Spalding, D., 1961. Measurements of entrainment by axisymmetrical turbulent jets. J. Fluid Mech. 11, 21.

Ruffin, E., Schiestel, R., Anselmet, F., Amielh, M., Fulachier, L., 1994. Investigation of characteristic scales in variable density turbulent jets using a second-order model. Phys. Fluids 6 (8), 2785–2799.

So, R., 1986. On self-preserving, variable-density, turbulent free jets. J. Appl. Math. Phys. 37, 538–558.

Sreenivasan, K., Raghu, S., Kyle, D., 1989. Absolute instability in variable-density round jets. Exp. Fluids 7, 309–317.

Stanley, S., Sarkar, S., 2000. Influence of nozzle conditions and discrete forcing on turbulent planar jets. AIAA 38, 1615–1623.

Stanley, S.A., Sarkar, S., Mellado, J.P., 2002. A study of the flowfield evolution and mixing in a planar turbulent jet using direct numerical simulation. J. Fluid Mech. 450, 377–407.

Thring, M.W., Newby, M.P., 1953. Combustion length of enclosed turbulent jet flames. In: Fourth Symposium (Intl.) on Combustion, pp. 789–796.

Tyliszczak, A., Boguslawski, A., 2006. Les of the jet in low mach variable density conditions. Direct and Large-Eddy Simulation VI, Part XII, pp. 575–582.

Vreman, B., Guerts, B., Kuerten, H., 1997. Large-eddy simulation of the turbulent mixing layer. J. Fluid Mech. 339, 357–390.

Wang, P., Fröhlich, J., Michelassi, V., Rodi, W., 2008. Velocity near-field of variable density turbulent jets. Int. J. Heat Fluid Flow 29, 654–664.

Witze, P., 1974. Centerline velocity decay for compressible free jets. AIAA J. 12, 417.

Zhou, X., Luo, K., Williams, J., 2001. Study of density effects in turbulent buoyant jets using large-eddy simulation. Theor. Comput. Fluid Dyn. 15, 95–120.